Nyquist-WDM Channel Generation using an Arrayed Waveguide Grating Router

Yiwei Xie, Leimeng Zhuang, Chen Zhu, and Arthur James Lowery
Electro-Photonics Laboratory, Dept. Elec. and Comp. Syst. Eng., Monash University, VIC 3800, Australia
Email: arthur.lowery@monash.edu

Abstract: We propose a method for generating Nyquist sinc pulses, based on an arrayed waveguide grating router (AWGR) preceded by a multimode interference coupler. This outperforms previous methods using a chirped AWGR and a dispersive fiber.
OCIS codes: (060.4510) Optical communication; (060.4230) Multiplexing; (070.0070) Fourier optics and signal processing.

1. Introduction

Nyquist pulse shaping enables wavelength multiplexing with minimal guard bands to create Nyquist-WDM (N-WDM) [1]. Nyquist pulse shaping can be achieved either electrically [2] or optically [3]. Electrical methods provide guaranteed roll-offs, but require expensive and power-hungry high-speed digital to analog converters (DAC). Alternatively, optical filtering is able to realize a cost-effective and greener Nyquist pulse shaping [1,3], but with the achievable roll-off limited to typically 10% [3].

Arrayed waveguide grating routers (AWGRs) have been proposed and demonstrated to realize discrete time-Fourier transformation (FT), and so can be used to generate optical frequency division multiplexed (OFDM) signals [4, 5]. In [6], a chirped AWGR has been proposed to implement a fractional FT (FrFT), which produces *chirped* OFDM signals that can be converted to quasi N-WDM channels using a dispersive fiber (DF) [6]. However, we have shown that these channels have much wider spectra than necessary [6], so require larger guard bands for a given level of inter-channel-interference (ICI) when multiplexed into a N-WDM spectrum.

In this paper, we propose a new photonic circuit topology with an AWGR at its core for Nyquist pulse shaping, which does not require a DF and produces near-optimal spectra. Simulations show that the proposed device has 4-dB *Q*-factor over the AWGR-DF design [6] in a N-WDM system when the OSNR is 19 dB. Furthermore, our design has a high tolerance to practical implementation issues such as waveguide loss (0.17 dB penalty when the waveguide is 2 dB/cm for N-WDM systems) and variation of waveguide length (0.5 dB penalty when the variation of waveguide length is 0.6 μm for N-WDM systems).

2. Operational principles of the AWGR as a Nyquist pulse shaper

Figure 1(a) illustrates signal processing diagram using Satoshi & Cincotti's method (AWGR-DF) to generate quasi-Nyquist sinc pulses [6]; Fig. 1(b) shows our proposed method (Multimode interference coupler (MMI)-AWGR).

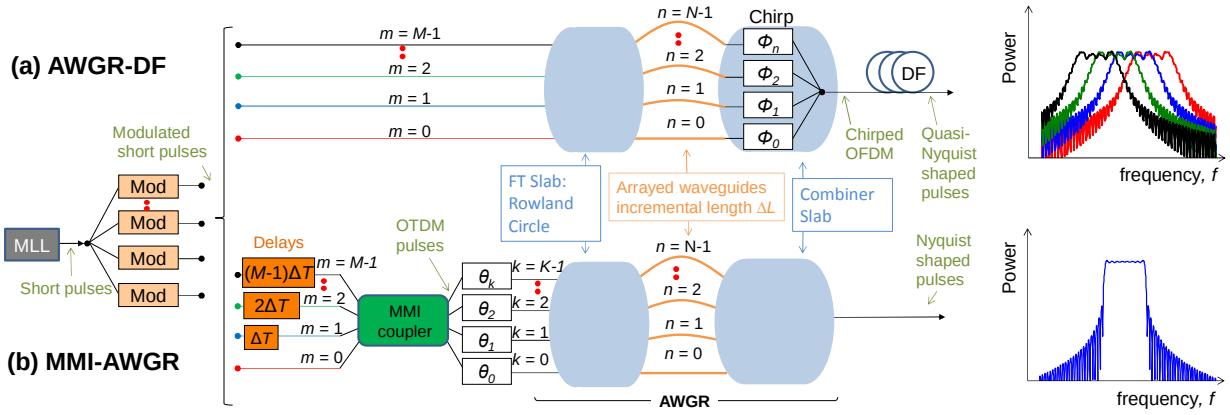

Fig. 1. Block diagrams for (a) AWGR-DF scheme [6] (top left) and (b) our proposed MMI-AWGR scheme (bottom left). The associated spectra are shown at the right-hand side.

In the AWGR-DF method, mode-locked laser (MLL) pulses are input to the first slab of an AWGR, which acts as a Fourier transform. The output of this slab is converted to a serial pulse stream using the differential delays of the waveguides, *n*. The second slab couples the outputs of the waveguide into a common output port, and also adds

quadratic phase shifts, to impose a linear chirp on the output pulses. A dispersive fiber (DF) compresses the chirped pulses into sinc-shaped pulses [7] and also imposes different time delays on each of the inputs pulses, to enable time-division multiplexing of the input pulses. Because each modulator feeds a separate input, *m*, of the first slab, each of these streams has a different central frequency. Therefore the output spectrum is a sum of these frequency-shifted spectra. This is wider than a conventional sinc-pulse's spectrum, as discussed in [1].

Figure 1(b) shows our proposed MMI-AWGR scheme. The input of the FT slab is fed with optically time-division multiplexed (OTDM) pulses created by splitting, modulating, delaying and then combining the MLL pulses. Again, the first slab of the AWGR is configured as a Rowland circle (RC), in which the phase shifts across it are proportional to $m \times n$. This implements the phase weighting of the discrete inverse FT [5]. The *N* outputs of the FT slab feed the arrayed waveguides, which act as a parallel-to-serial converter.

For the AWGR to output a truncated sinc-like pulse, its inputs need to have uniform powers and precise phases. In practice, its input waveguides, which representing the frequency coefficients into the inverse FT, should be fed with identical and synchronized signal copies from the same modulated source. In this case, these input pulses can be derived by equally splitting an input signal, which is a data-modulated pulse train, using a multimode interference coupler (MMI). Thus, if OTDM pulses from a MLL are input to a FT slab, the spatial distribution at the output plane of the FT slab will be a truncated-sinc. This assumes that the inputs of the FT slab have the same phase and amplitude, and the transmission from any input waveguide to output waveguide of the slab has identical losses; that is, for every combination of *m* and *n*. The arrayed waveguides rearrange these space samples in sequence at the combiner, because each waveguide has an incremental path length ΔL, the output is a sampled truncated sinc pulse waveform, with a duration dependent on the number of arrayed waveguides, *N*, and the incremental delay of the arms, Δt.

For the proposed scheme as shown in Fig. 1(b), as each input of the FT slab produces a sinc spectrum with a different central frequency at the output of the second slab, the transfer function is:

$$H(f) = \sum_{k=0}^{K-1} \mathrm{sinc}\left[\frac{\left(f - k \cdot \Delta f\right)}{\Delta F}\right] = \sum_{k=0}^{K-1} \mathrm{sinc}\left[\left(f - k \cdot \Delta f\right) N \Delta t\right] \quad (1)$$

Thus, we can easily find the frequency spectrum as a summation of sinc spectra with widths ΔF, each shifted by Δf, over the number of input, *K*, lines. From Eq. (1), the roll-off factor of the spectrum depends on the width of the sinc subcarriers' spectra; thus, the smaller the ΔF is, the smaller the roll-off factor becomes. Here the roll-off is defined as the width of the sinc spectra divided by the bandwidth of the spectrum.

3. Simulation results

Figure 2(a) shows the schematic of a 3-channel N-WDM transmission system that we simulated with VPItransmissionMaker. The MLL's output was split into three paths, each leads to a 160-Gbaud N-OTDM channel with 16 10-Gbaud QPSK tributaries. The width, ΔT, of the Nyquist pulses is designed to be 6.25 ps with a spectral bandwidth B = 160 GHz, for consistency with our theoretical paper [1]. The parameter values for the structural design of the AWGR are listed in Table 1. Each N-WDM channel uses a 240-GHz Gaussian 1st-order band-pass filter (BPF) to remove energy from the higher-order passbands of the MMI-AWGR to build a N-WDM spectrum. The receiver used a BPF with a 160-GHz Gaussian 2nd-order response to select the central channel.

Figure 2(b) compares the signal quality versus OSNR for a single wavelength channel to that of the central channel in a 3-channel N-WDM system with no frequency guard bands (160-GHz spacing) for AWGR-DF [6] and the proposed MMI-AWGR scheme. From Fig. 2(b), the N-WDM system using AWGRs-DFs suffers a much greater penalty (6 dB) than the MMI-AWGR (2 dB), compared with an ideal single-channel system when the OSNR = 19 dB. Fig. 2(c) shows that the *Q*-factor becomes OSNR-limited when the guard band is 12 GHz for the MMI-AWGR, which is 75% narrower than required for AWGR-DF design. This also outperforms our previous modified AWGR-DF, as that needed 50-GHz guard-bands to reduce the ICI to insignificance at 20-dB OSNR [1].

Fig. 3 plots the fabrication tolerance of arm loss and waveguide length variation for the central WDM channel (160-GHz spacing) with different numbers of arrayed waveguides, *N*. On one hand, a greater *N* reduces the ICI; on the other hand, even with a large waveguide loss of 2 dB/cm, the performance drops only 0.17 dB. The *Q*-factor is reduced by 0.5 dB when the standard deviation of the waveguide length reaches 0.6 μm, for OSNR = 19 dB.

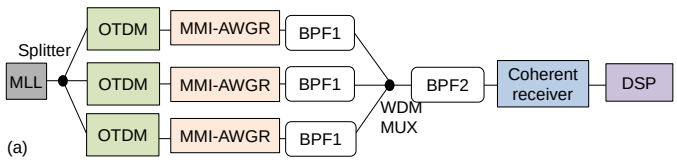

Table 1 Parameters used in the design of AWGR

Number of the FT slab inputs	K	16
Number of arrayed waveguides	N	101
Spacing between input waveguides of FT slab	d	26.5 μm
Spacing between arrayed waveguides	D	24.2 μm
Focal length of the FT slab	R	60 mm
Differential arrayed waveguides length	ΔL	0.2 mm
Refractive index of the FT slab and waveguides	n_s	1.45

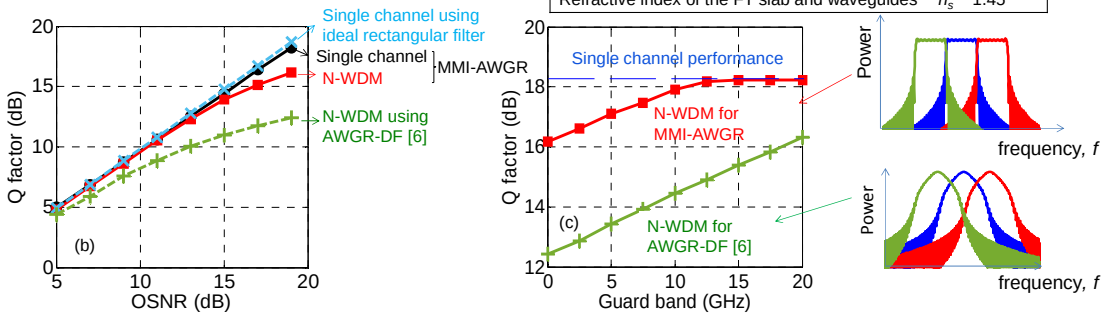

Fig. 2. (a) Schematic diagram for N-WDM using AWGRs. (b) Comparison of the *Q*-factors for single channel and N-WDM using two schemes. (c) The *Q*-factors for three WDM channels with respect to guard band using two schemes (OSNR = 19 dB). (DSP: digital signal processing)

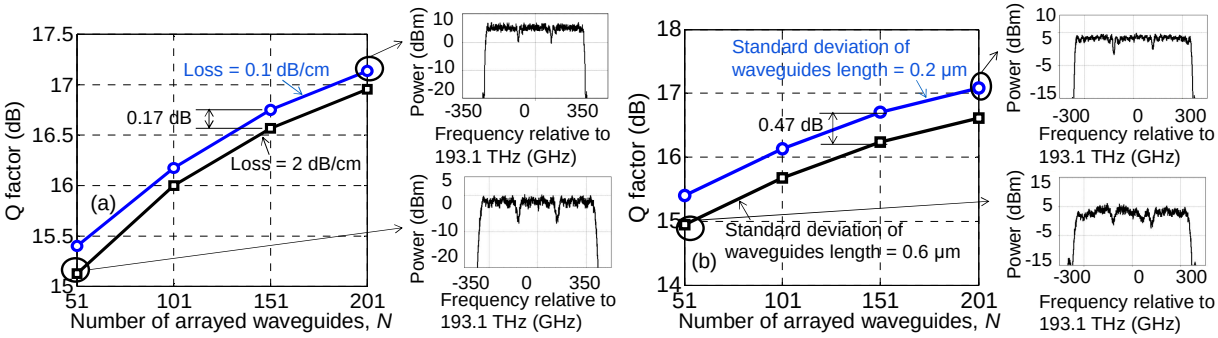

Fig. 3. The influence of: (a) the arm loss and (b) arrayed waveguides length variation for N-WDM systems with respect to the number of waveguides (OSNR = 19 dB).

4. Conclusions

We have proposed a method of shaping pulses to have spectra suitable for Nyquist-WDM systems, which is suitable for manufacture using planar-waveguide technology. Because of its narrow output spectrum, it has 4-dB better performance than an earlier proposal using a chirped AWGR followed by a dispersive fiber.

Acknowledgements

We thank VPIphotonics for the use of their simulator, VPItransmissionMakerWDM V9.5. This work is supported under the Australian Research Council's Laureate Fellowship scheme (FL 130100041).

References

[1] A. J. Lowery, *et al*., "Systems performance comparison of three all-optical generation schemes for quasi-Nyquist WDM," Opt. Expr. **23**(17), 21706-21718 (2015).
[2] R. Cigliutti, *et al*., "Ultra-long-haul transmission of 16x112 Gb/s spectrally-engineered DAC-generated Nyquist-WDM PM-16QAM channels with 1.05 x (symbol-rate) frequency spacing," OFC 2012, paper OTh3A.3.
[3] T. Hirooka, *et al*., "Highly dispersion-tolerant 160 Gbaud optical Nyquist pulse TDM transmission over 525 km," Opt. Expr. **20**(14), 15001-15007 (2012).
[4] A. J. Lowery, "Design of arrayed-waveguide grating routers for use as optical OFDM demultiplexers," Opt. Expr. **18**(13), 14129-14143 (2010).
[5] S. Shimizu, *et al*., "Demonstration and performance investigation of all-optical OFDM systems based on arrayed waveguide gratings," Opt. Expr. **20**(26), B525-B534 (2012).
[6] G. Cincotti, "Enhanced functionalities for AWGs," J. Lightw. Technol. **33**(5), 998-1006 (2015).
[7] D. Yang, and S. Kumar, "Realization of optical OFDM using time lenses and its comparison with optical OFDM using FFT," Opt. Expr. **17**(20), 17214-17226 (2009).